Characterization of TWIK-2, a Two-Pore Domain K^+ Channel, Cloned from the Rat Middle Cerebral Artery

ERIC E. LLOYD,* SEAN P. MARRELLI,*,†,‡ KHODADAD NAMIRANIAN,*,‡ AND ROBERT M. BRYAN, JR.*,†,‡,§,[1]

Department of Anesthesiology; †Department of Molecular Physiology and Biophysics; ‡Graduate Program in Cardiovascular Sciences; and §Department of Medicine (Cardiovascular Sciences), Baylor College of Medicine, Houston, Texas 77030

TWIK-2, a member of the Two-Pore Domain K channel family, is expressed in a number of mammalian tissues including the vascular system. The function of TWIK-2 is not known. The purpose of this study was to clone the TWIK-2 channel from the rat middle cerebral artery, express it in CHO cells, and characterize the channel's electrical properties. In light of the fact that there are no specific TWIK-2 inhibitors or activators, a better characterization of the channel should enhance our understanding of its role in the vascular system. TWIK-2 was cloned from the rat middle cerebral artery and expressed with an N-terminal green fluorescence protein (GFP) in CHO cells. We report that rTWIK-2-GFP currents were relatively linear at physiological K^+ concentrations but become slightly inwardly rectifying in symmetrical K^+. rTWIK-2-GFP was insensitive to 10 mM TEA, 3 mM 4-aminopyridine, and 10 μM glibenclamide. However, rTWIK-2-GFP was inhibited by Ba^{2+} with 50% of the current being blocked at 80 μM. rTWIK-2-GFP activity was enhanced 60% by 100 μM arachidonic acid. The electrophysiological characteristics of TWIK-2 indicate that it could serve an important role in ion homeostasis and regulation of the membrane potential in arteries and arterioles. Exp Biol Med 234:1493–1502, 2009

Key words: cerebral circulation; potassium channels; two-pore domain potassium channels

Introduction

A major role of potassium or K channels in the vascular system is to control blood flow by regulating the diameter of arteries and arterioles. When K channels open during normal physiological conditions, K^+ moves along its electro-chemical gradient from the cytoplasmic space to the extracellular space. The loss of positive K ions hyperpolarizes the membrane. In vascular smooth muscle (VSM) this hyperpolarization closes voltage-dependent calcium channels, and decreases intracellular free Ca^{2+}. Since cytoplasmic free Ca^{2+} is a second messenger for VSM contraction, the net result of K channel activation is relaxation of VSM and vessel dilation. Conversely, when K channels close, intracellular free Ca^{2+} increases as a result of voltage-dependent calcium channel activation and vessels constrict.

K channels from three families are expressed by VSM and serve to regulate the vascular tone (1–5). These three families are characterized by the number of transmembrane spanning domains for each protein subunit. A family of two transmembrane spanning domains for each protein subunit includes inwardly rectifying and ATP-sensitive K channels. A second family having six or seven transmembrane spanning domains for each protein subunit includes the voltage-gated and Ca^{2+}-activated K channels. Both of the above families have one pore domain, the site where K moves through the channel. Four subunits and, thus, four pore domains, are required to form a fully functioning K^+ channel. The most recent family of K channels to be discovered is characterized by four transmembrane spanning domains and two pore domains for each protein subunit. Members of this latter family are coded by 15 genes (*KCNK*) and have been given the name Two-Pore Domain K channels (K_{2P}). Unlike the other two families, only two protein subunits, each contributing two pore domains, are required to form a fully functional channel. Cerebral and peripheral arteries express a number of the K_{2P} and some of

This work was supported by grants RO1 NS-46666 (RMB), PO1 NS-038660 (RMB), RO1 HL-088435 (SPM), grant 0665100Y from the American Heart Association (SPM), and a Predoctoral Fellowship 0815342F from the South Central Affiliate of the American Heart Association (KN).

[1] To whom correspondence should be addressed at Department of Anesthesiology, Room 434D, Baylor College of Medicine, One Baylor Plaza, Houston, TX 77030. E-mail: rbryan@bcm.edu

Received March 17, 2009.
Accepted July 21, 2009.

DOI: 10.3181/0903-RM-110
1535-3702/09/23412-1493$15.00

these have been shown to regulate vascular tone (6–12) [for review see (3)].

One of the K_{2P}, TWIK-2 (***T***andem of P domains in a ***W***eak ***I***nward rectifying ***K*** channel) is especially abundant in the vasculature (6, 7, 13). To date, very little is known about TWIK-2 in general and virtually nothing is known about its function in the vasculature. There have been four published studies where TWIK-2 was cloned (13–16) [note that one study (15) gave the name TOSS to the channel which is now commonly referred to as TWIK-2]; however, only two of these studies were able to demonstrate functional channels when heterologously expressed (13, 14). When functional channels could not be demonstrated, it is likely that the channels were synthesized but not incorporated into the membrane (15, 16).

In the first study showing functional channels, TWIK-2 was cloned from a human brain cDNA library and expressed in *Xenopus* oocytes (14). In the second study showing functional channels, TWIK-2 was cloned from human brain and rat heart libraries and expressed in COS cells (13). Of significance, there are a number of discrepancies in the electrophysiological properties for TWIK-2 as described by the two groups (13, 14). The discrepancies include differences in rectification, inactivation, sensitivity to arachidonic acid, and sensitivity to Ba^{2+} (13, 14).

Given the existing discrepancies in the channel properties for TWIK-2, additional studies identifying their characteristics are warranted. The purpose of this study was to clone the TWIK-2 channel from the rat middle cerebral artery, express it in CHO cells, and characterize its electrical properties. In light of the fact that there are no specific inhibitors or activators, a better understanding of the channel characteristics should provide a better understanding of its role in the vascular system. A common strategy for studying other K_{2P}, which lack specific pharmacological tools, is to compare currents from the cloned channels to currents in native cells (17, 18). Therefore, we also compared the channel characteristics of the cloned TWIK-2 to native channels in VSM of rat middle cerebral artery (6) with the idea of better determining the role for TWIK-2 in regulating K^+ current and vascular tone.

Materials and Methods

Cloning and Expressing TWIK-2 from the Rat Middle Cerebral Artery. One male Long Evans rat was anesthetized with 3% isoflurane and decapitated. The brain was immediately removed from the skull and placed in chilled Ringer's solution. Both the left and right middle cerebral arteries (MCA) were carefully dissected, snap frozen in liquid nitrogen, and homogenized. Total RNA was extracted using a Qiagen Micro RNA Isolation Kit according to the manufacturer's instructions. Strands of RNA containing a poly-A sequence were purified and separated from the total RNA pool using an Oligotex mRNA Miniprep Kit (Qiagen). The mRNA was reverse transcribed using oligo dT primers (SuperScript III, Invitrogen). The cDNA was amplified by PCR (30 cycles) using *Pfu* DNA polymerase (Invitrogen) and primers for rat KCNK6 (TWIK-2) which spanned the coding region. The primers were as follows: (Forward) ATGCGGCGGGGC GCGCTCCTGGCT and (Reverse) GATCCTACCTGG GGATGGAGGCGTAATT.

The PCR products were separated using electrophoresis and visualized with ethidium bromide and UV illumination. The product showed a band at the predicted size for the TWIK-2 coding region (942 bp). This putative TWIK-2 band was gel purified and adenine was added to the 3' end of the cDNA (3'-A-tailed). The cDNA was TA cloned into the pGEM-T Easy Vector (Promega). The clone was sequenced and validated to be TWIK-2.

The coding region of TWIK-2 was subcloned into the donor vehicle pDNR (BD Biosciences). Through mediated recombination, the TWIK-2 coding region was transferred into one of two expression plasmids using the Creator Cloning Kit (BD Biosciences). One plasmid (pLP-CMV) used an untagged version of TWIK-2, and the other plasmid (pLP-AcGFP1-C) placed a green fluorescence protein (GFP) tag at the N-terminus of TWIK-2. Initially we attempted to conduct electrophysiological studies using the non-tagged rTWIK-2. However, we determined that in order to effectively select a cell for study, we needed to know that rTWIK-2 was expressed in that cell and that the channels were inserted into the plasma membrane. Hence, the GFP containing rTWIK-2 was used for recording currents.

In order to create stable cells lines we linearized the TWIK-2 construct with SpeI (New England Biolabs) and transfected it into CHO-K1 cells using Lipofectamine 2000. A single neomycin-resistant cell was grown into a colony and less than 10 passages were used for all experimentation. Endotoxin-free maxi preparations (Qiagen) were used to create a transfectable stock of plasmid DNA.

In order to validate cell surface expression, we separated the membrane fraction of TWIK-2 expressing cells from the cytoplasmic fraction using the EZ-Link sulfo-NHS-biotin Kit (Pierce). Briefly, the membrane fraction was isolated using a Zeba Desalt Spin Column (Pierce) after biotinylating surface proteins.

Western Blot. Cells were minced on ice and homogenized in buffer containing 1% SDS (Bio-Rad), and protease inhibitor cocktail (Complete Mini, Roche).

Samples were boiled for 15 min and centrifuged at 15,000 *g* for 15 min, and the supernatant was collected for protein analysis using the DC protein assay (Bio-Rad). Protein samples (5 μg/lane) were size fractionated by electrophoresis for 1 h using 90 V at room temperature with a 7.5% tris-glycine gel. Proteins were transferred to a PVDF Membrane. The blots were blocked with PBS containing 5% nonfat dry milk with 0.1% Tween 20 for 1 h at room temperature and subsequently probed with 10 μg/ml anti-TWIK-2 (Alomone) in blocking solution. Membranes were washed (3 × 20 min) in PBS and probed with goat anti-

rabbit horseradish peroxidase-conjugated secondary antibody (1:10,000 dilution; Pierce) for 1 h at room temperature. Blots were incubated in chemiluminescent substrate (Pierce Femto kit) for 5 min at room temperature and exposed to film (Hyperfilm ECL, Amersham Biosciences).

Live Imaging of CHO Cells. Cells were imaged live to evaluate the expression pattern of rTWIK-2-GFP. Briefly cells were exposed to H33342 nuclear stain (Molecular Probes) at 37°C for 20 min and placed on the stage of a Nikon TE2000-U microscope. The images were collected at a number of planes, which were 0.2 μm apart, using MetaVue Software (v 6.2r4, Molecular Devices, Downington, PA) and processed with a deconvolution algorithm (AutoDeblur + AutoVisualize, v 9.3, Media Cybernetics, Inc., Bethesda, MD).

Electrophysiological Studies. CHO-K1 rTWIK-2-GFP expressing and non-expressing control cells were trypsin-digested and plated on #1 cover slips. The cover slips had been previously baked at 180°C for > 24 h and coated with poly-L-lysine. The cover slips containing the cells were incubated in culture media (F12 with 10% heat-inactivated FBS) for 48 to 72 h. For electrophysiological studies, the cover slips containing the cells were placed in a chamber on the stage of an inverted microscope (Nikon TMS) and continually superfused with buffer. Whole cell currents from individual CHO cells were measured using an Axopatch 200B amplifier and pCLAMP 9.2 software (Axon Instruments, Union City, CA). Data were filtered at 2 kHz with a four-pole Bessel filter and stored on a hard disk. There was no compensation for cell capacitance, series resistance, or leak current. The liquid junction potential was calculated using pClamp and corrected. Currents are expressed as picoamperes (pA) or current density [pA/membrane capacitance] to normalize for differences between cell membrane areas. The membrane capacitance (pF) of each cell was calculated with the pCLAMP software by dividing the charge produced during a pulse by the pulse voltage. Patch electrodes were pulled from glass tubing (catalog no. 2-000-210, Drummond Scientific) in two stages using a pipette puller (model PP-830, Narishige) and polished with a microforge (model MF-830, Narishige). Pipette resistances were 2–3 MΩ. The pipette buffer consisted of (in mM) 100 gluconate (K^+ salt), 43 KCl, 1 $MgCl_2$, 0.1 EGTA, and 10 HEPES; pH was adjusted to 7.2 with KOH. The bath buffer contained (mM) 137 NaCl, 5.6 KCl, 1 $MgCl_2$, 0.1 $CaCl_2$, 5 glucose, and 10 HEPES; pH was adjusted to 7.4 with NaOH. In one study, the K^+ concentration was increased to 30 and 140 mM. In each case, Na^+ concentration was reduced in an equimolar amount.

Whole cell currents were measured after rupturing the patch using negative pressure applied to the pipette. Cells were held at −70 mV prior to initiation of pulse or ramp protocols. For the pulse protocol, a family of currents was generated where Vm was shifted from the holding potential to −120 mV for 500 msec followed by progressive 10-mV steps (500 msec, 5-s interval) from −120 to 100 mV (Fig. 2A). For the ramp protocol Vm was changed to −120 mV and ramped to 100 mV over a period of 1 sec (Fig. 2B).

Materials. Lipofectamine 2000, trypsin, F12 media, and FBS were obtained from Invitrogen. Poly-lysine, tetraethylammonium, 4-aminopyridine, glibenclamide, barium chloride, and arachidonic acid (sodium salt) were purchased from Sigma. Arachidonic acid was dissolved in ethanol.

Data Analysis and Statistical. Concentration effects of extracellular Ba^{2+} on the rTWIK-2-GFP current were fit to a Hill equation:

$$I_{Ba2+}/I_{Control} = 1 \Big/ \left[1 + ([Ba^+]/IC_{50})^h\right] \qquad (1)$$

using the Levenberg-Marquardt algorithm where I_{Ba2+} is the current after Ba^{2+}, $I_{Control}$ is the current in the control (absence of Ba^{2+}), $[Ba^{2+}]$ is the extracellular concentration of Ba^{2+}, IC_{50} is the concentration of Ba^{2+} necessary to inhibit 50% of the response, and h is the Hill coefficient. Data are expressed as the mean ± standard error of the mean. For statistical analysis, the two-way repeated measures analysis of variance, followed by Student-Newman-Keuls post-hoc test, when appropriated, was used for analysis of the current-voltage data. $P < 0.05$ was defined as the acceptable level of significance.

Results

Our cloned TWIK-2 showed 100% homology to the published rTWIK-2 [NCBI accession # NM_053806.1 (942 base pairs)]. Figure 1A shows CHO cells expressing rTWIK-2-GFP (green) at 24, 48, and 72 h after passage. rTWIK-2-GFP first appeared in a punctate pattern around the nuclei (blue) at 24 h and progressively moved towards the cell surface over time. Note that there were cells that did not express rTWIK-2-GFP as indicated by the H33342 nuclear dye (blue) not associated with surrounding green fluorescence. Figure 1B shows a Western blot, which was probed with an anti-TWIK-2 antibody, in non-expressing (control) and rTWIK-2-expressing CHO cells. Note the single band in the lane representing the rTWIK-2-expressing CHO cells which was absent in the non-expressing control cells. The band at approximately 35 kDa is in good agreement with the predicted size of the theoretical of 34 kDa for rat TWIK-2 [NP_446258.2 (313 amino acids) (NCBI database)].

Figure 1C shows Western blots for the membrane and lysate fractions of non-expressing control CHO cells (lanes 1 and 3) and rTWIK-2-GFP expressing CHO cells (lanes 2 and 4). Note the band shift when GFP was fused with TWIK-2 (Fig. 1C) compared to rTWIK-2 alone (i.e., no GFP, Fig. 1B). rTWIK-2-GFP was present in both the cell lysate and membrane fraction as would be predicted by protein distribution shown in Figure 1A (72 h). The presence in the membrane fraction indicates that not only

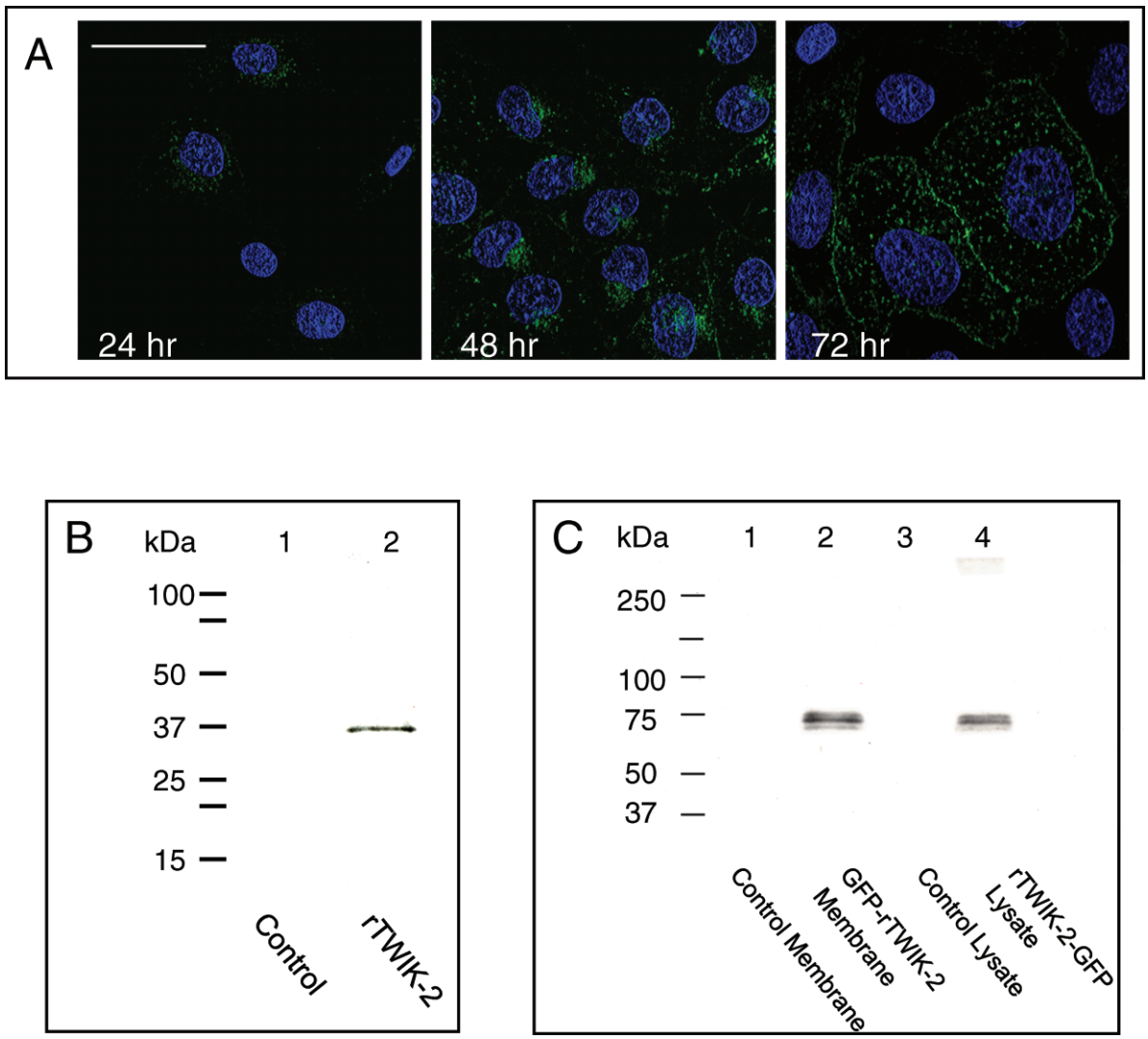

Figure 1. (A) Live image of rTWIK-2-GFP (green) expressed in CHO cells at 24, 48, and 72 h after passage. The blue color (H33342) represents nuclei. Bar = 50 μM. (B) Western blots showing expression of rTWIK-2 in expressing but not in non-expressing control CHO cells. (C) Western blot of rTWIK-2-GFP of membrane and lysate fractions in rTWIK-2-GFP expressing cells (lanes 2 and 4, respectively) and in non-expressing control cells (lanes 1 and 3, respectively).

was rTWIK-2-GFP expressed in CHO cells but it is also inserted into the plasmalemma. The non-expressing control cells showed no band in either the membrane or lysate fraction.

Whole cell currents were measured in rTWIK-2-GFP expressing CHO cells. Having GFP fused to the rTWIK-2 was necessary for identifying cells where the channel was not only expressed but also identifying cells where it was inserted into the plasmalemma. Many cells that expressed rTWIK-2-GFP or rTWIK-2 did not insert the channel into the membrane. Figure 2A shows whole cell currents from a control cell (top) and an rTWIK-2-GFP CHO cell (bottom) using the pulse protocol (pictured in the insert). The current in the rTWIK-2-GFP expressing CHO cell was slightly inactivating at the more depolarized potentials. Figure 2B shows currents using a ramp protocol. For both the pulse and ramp protocols, currents in the rTWIK-2-GFP expressing cells were greater than that in the controls. Figure 2C shows the mean data using the pulse protocol for 30 rTWIK-2-GFP expressing cells and 19 controls. Statistical analysis using the two-way repeated measures ANOVA shows that there is significant group difference between genotype (i.e., control and rTWIK-2-GFP expression) ($P < 0.001$) and a significant interaction between the genotype and membrane potential (mV, $P < 0.001$). The reversal potential for control and rTWIK-2-GFP expressing cells were -45 ± 4 ($n = 19$) and -78 ± 1 ($n = 30$), respectively ($P < 0.001$ using t test).

In a physiological K^+ gradient (5.6 and 143 mM K^+ extracellular and intracellular, respectively), the currents were near linear or very slightly outwardly rectifying (Figs. 2B, 2C, and 3A). When extracellular K^+ was increased to 30 and 140 mM the currents in rTWIK-2-GFP expressing CHO cells shifted to the right and became slightly inwardly rectifying (Fig. 3A, $n = 5$ for each K^+ concentration). Note

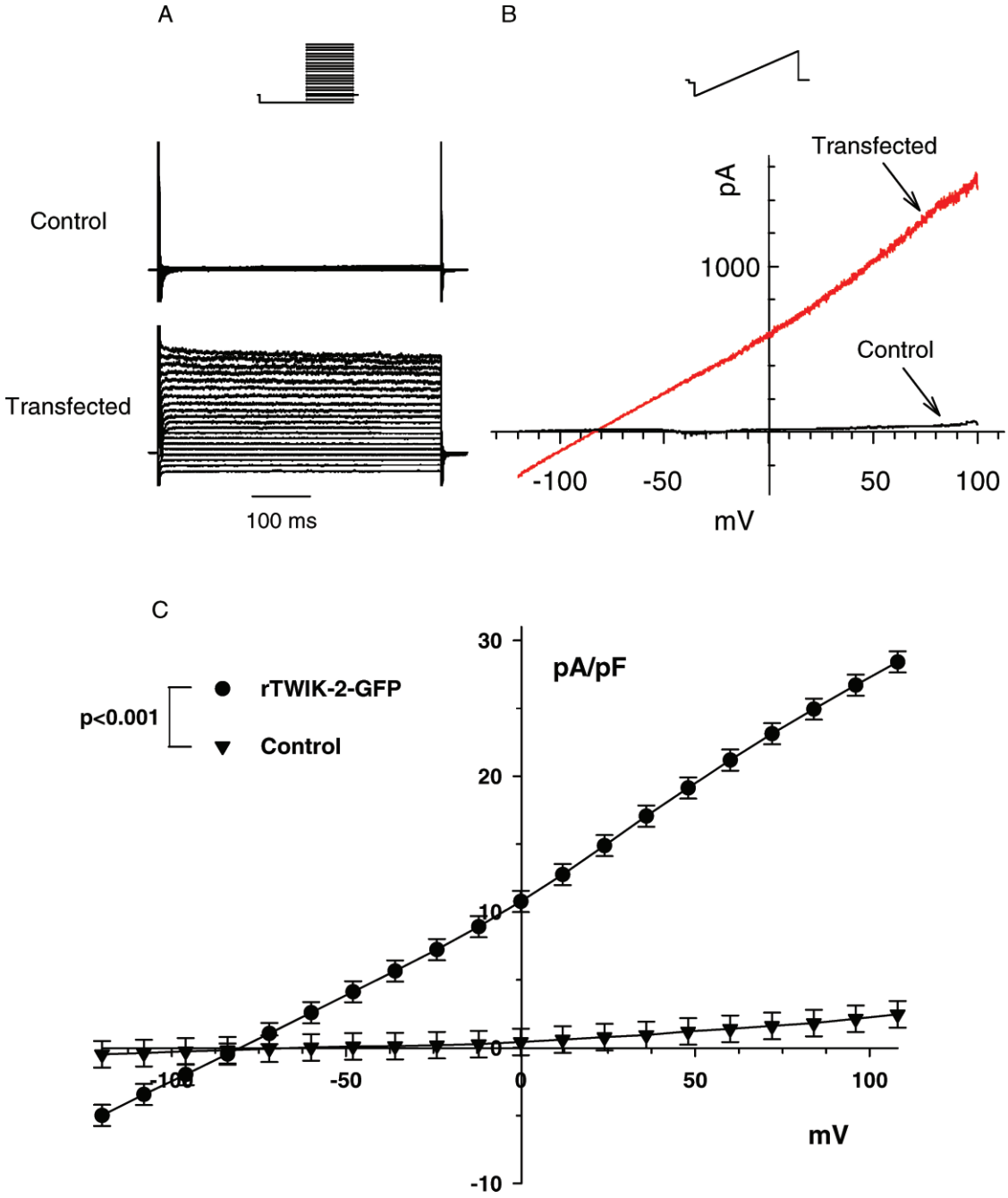

Figure 2. (A) Whole cell currents from a control (top) and an rTWIK-2-GFP expressing CHO cell (bottom) using the pulse protocol. (B) Whole cell currents from a control and a rTWIK-2-GFP expressing CHO cell recorded using the ramp protocol. (C) Mean whole cell currents recorded from 19 control and 30 rTWIK-2-GFP expressing CHO cells using the pulse protocol. The current (Y axis) has been normalized to the membrane capacitance (pF). A color version of this figure is available in the online journal.

the reversal potential (the membrane potential where the current = 0) shifted to more positive values as would be predicted for a K channel with an increasing concentration of extracellular K^+ and constant intracellular K^+. Two-way repeated measures ANOVA reveals a significant effect due to extracellular K^+ ($P < 0.001$, $n = 5$ for each concentration of extracellular K^+) and a significant interaction between extracellular K^+ and membrane potential (mV, $P < 0.001$). Figure 3B shows a semi-log plot of the reversal potential as a function of extracellular K^+. Note that the experimentally determined reversal potential is close to the theoretical relationship (dashed line), which was calculated from the Nernst equation, for K^+ as the current carrier. The linear equation describing the experimentally determined relationship between reversal potential and extracellular K^+ is:

$$\text{Reversal Potential} = -66.8 + 0.5[\text{K}]$$

where K^+ concentration in mM is [K] ($P < 0.001$ for

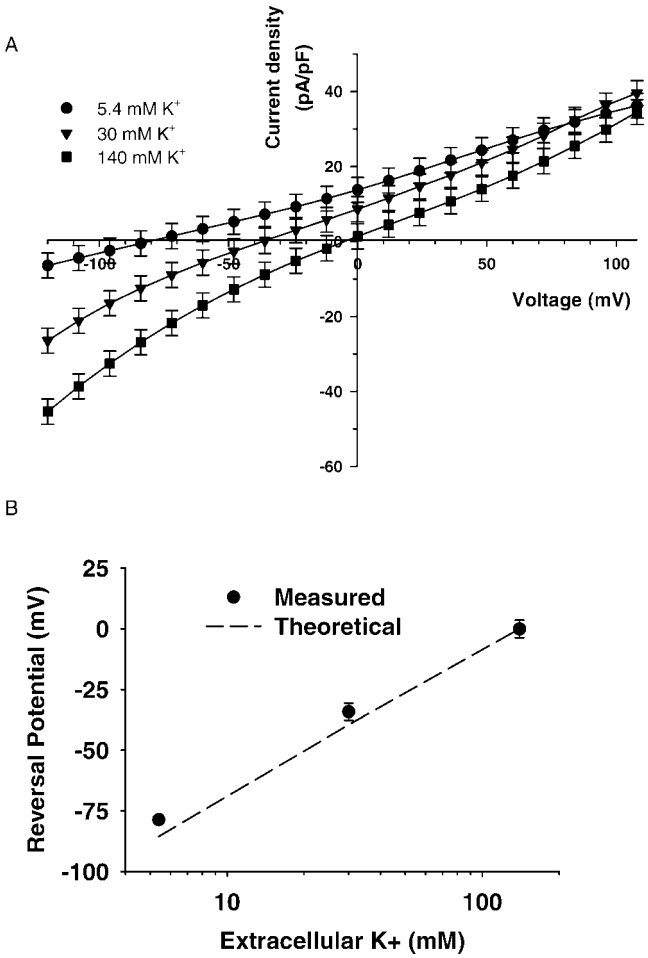

Figure 3. (A) Whole cell currents in rTWIK-2-GFP expressing CHO cells with extracellular K^+ concentrations of 5.4, 30, or 140 mM ($n = 5$ for each K^+ concentration). (B) Plot of the reversal potential as a function of the log of extracellular K^+. The dashed line is the theoretical plot if K^+ is the sole current carrier.

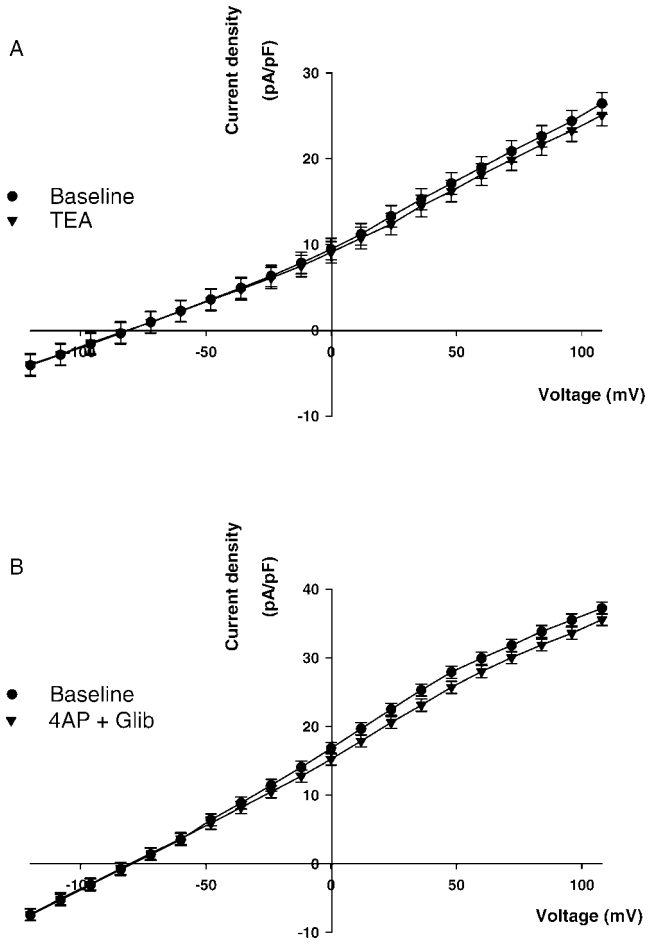

Figure 4. Whole cell currents in rTWIK-2-GFP expressing CHO cells before and after 10 mM TEA ($n = 6$) (A) or before and after a combination of 3 mM 4-aminopyridine (4AP) and 10 μM glibenclamide (Glib, $n = 3$) (B).

constant, $P < 0.001$ for [K], and r^2 adjusted = 78.8%). This compares favorably to the predicted equation if K^+ is the sole current carrier:

$$\text{Predicted Reversal Potential} = -73.9 + .551[\text{K}]$$

We determined the effects of TEA, 4-aminopyridine, and glibenclamide, inhibitors of Ca^{2+}-activated, voltage-gated, and ATP-sensitive K channels, respectively, on rTWIK-2-GFP currents. Figure 4 demonstrates that rTWIK-2-GFP was not inhibited by 10 mM TEA (panel A, $P = 0.249$, $n = 6$) or a cocktail containing 3 mM 4-aminopyridine and 10 μM gilbenclamide (panel B, $P = 0.16$, $n = 3$).

Figure 5A shows the effects of Ba^{2+} on rTWIK-2-GFP current in an individual CHO cell. The summary data for the Ba^{2+} effect is shown in Figure 5B. At a concentration of 10 μM Ba^{2+}, no significant effect could be seen. However, at higher concentrations (100 and 1000 μM), Ba^{2+} inhibited the rTWIK-2-GFP current. Two-way repeated measures ANOVA revealed a significant effect due to Ba^{2+} concentration ($P < 0.001$) and a significant interaction between Ba^{2+} concentration and membrane potential (mV, $P < 0.001$, $n = 5$ per group). Using the post-hoc Student-Newman-Keuls test, all groups were statistically different from one another ($P < 0.001$) with one exception. The Baseline, which did not receive Ba^{2+}, and the group receiving 10 μM Ba^{2+} did not show a statistically significant difference ($P = 0.133$). At 0 mV, 1000 μM Ba^{2+} inhibited current by 90 ± 1%.

The effect of Ba^{2+} on normalized currents ($I_{Ba2+}/I_{Control}$) at three potentials, –48, –36, and –24 mV, surrounding the physiological Vm are shown in Figure 6. The mean experimental data (± standard error of mean, $n = 5$) is depicted by the symbols and the lines represent the best fit to Equation 1 (see Methods). Calculated concentrations to inhibit 50% of the current (IC_{50}) for –48, –36, and –24 mV were 77 ± 7, 78 ± 7, 82 ± 7 μM ($n = 5$), respectively. The Hill coefficients were 1.7 ± 0.78, 3.9 ± 0.04, and 3.6 ± 0.27.

Activation of TWIK-2 by arachidonic acid may be responsible for dilations and increased VSM currents in the

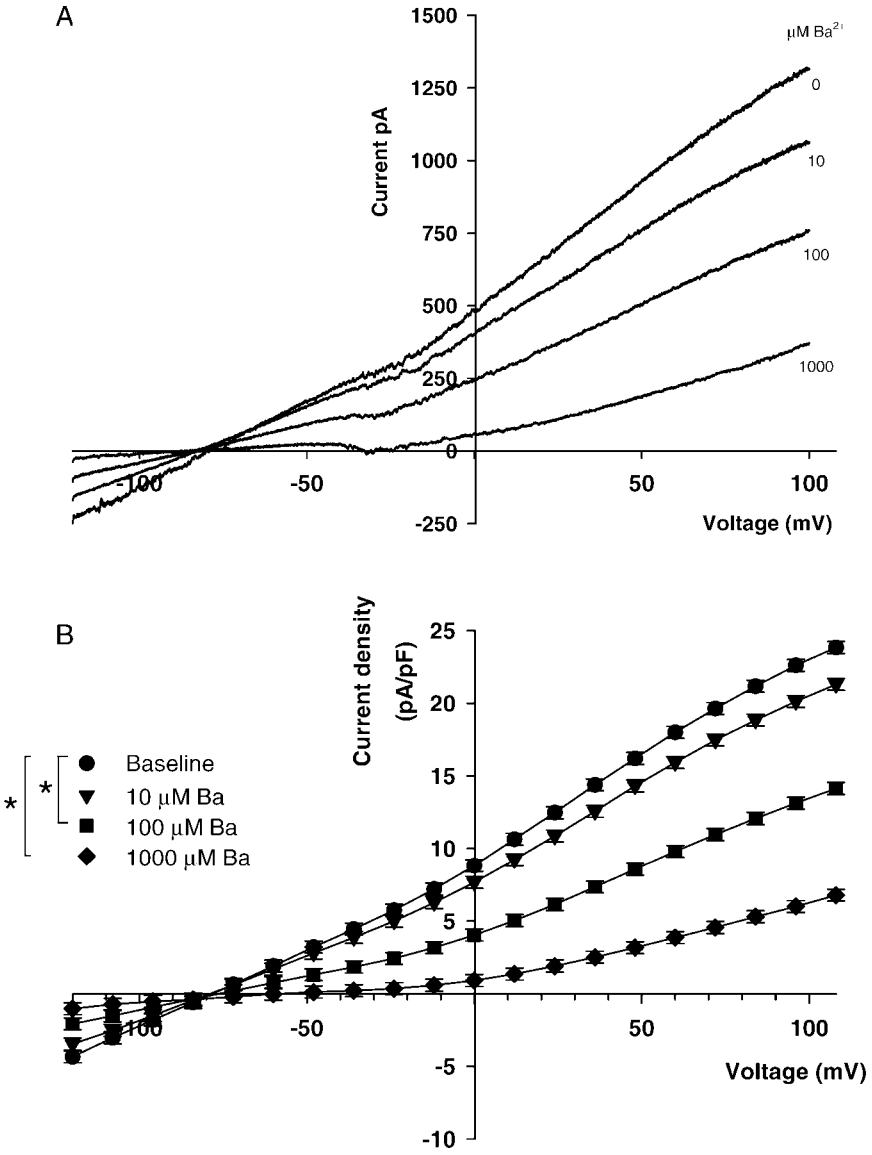

Figure 5. (A) Whole cell current in an rTWIK-2-GFP expressing CHO cell before and after 10, 100, or 1000 μM Ba^{2+}. (B) Summary data for Ba^{2+} inhibition of rTWIK-2-GFP ($n = 5$ per group). All groups were statistically significant from one another ($P < 0.001$) with one exception (Baseline versus 10 μM Ba^{2+}). Two of these comparisons are depicted in the figure legend; * $P < 0.001$ between groups.

rat middle cerebral artery (6). Therefore, we determined the effects of arachidonic acid on rTWIK-2-GFP currents. The effects of arachidonic acid (AA) on a single TWIK-2-expressing CHO cell is shown in Figure 7A with the summary data in Figure 7B ($n = 4$–6). Addition of 10 μM AA had no significant effect on currents; however, 100 μM AA increased rTWIK-2-GFP currents compared to the corresponding baseline current. Two-way repeated measures ANOVA showed a significant interaction between AA concentrations and membrane potential (mV, $P < 0.001$). The interaction between AA concentration and membrane potential allowed for individual comparisons using Student-Newman-Keuls. AA (100 μM) significantly increased rTWIK-2-GFP currents at the more positive potentials. At 48 mV the currents produced by 100 μM AA increased by 59 ± 17% ($n = 4$). AA had no effect on current in the non-expressing cells at either 10 or 100 μM AA (data not shown).

Discussion

The discovery of the K_{2P} channel family is based on the fact that all known K channels share a pore forming region or P domain which is highly conserved across species (19). A search of the human genome for DNA sequences coding for the P domain led to the first K_{2P} to be identified and cloned (20). The channel was named TWIK-1, an acronym for ***T***andem of P domains in a ***W***eak ***I***nward rectifying ***K*** channel. Since the initial discovery, a total of 15 genes have been discovered and classified in order of discovery using the gene name *KCNK* (21).

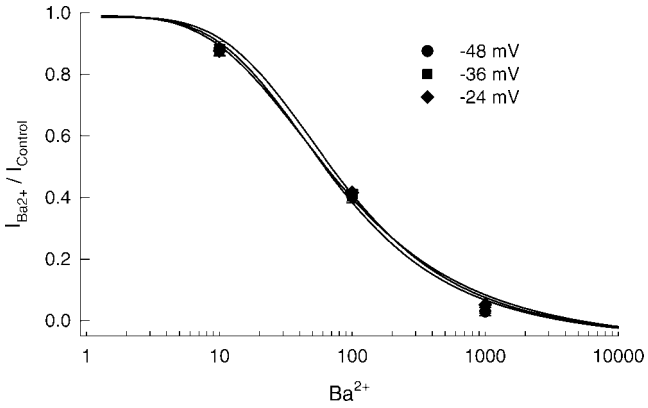

Figure 6. The effect of Ba^{2+} on normalized currents ($I_{Ba2+}/I_{Control}$) ($n=5$) at three potentials near the normal physiological potential. The lines represent the best fit to Equation 1 (see Methods). The Hill coefficients were 1.7 ± 0.78, 3.9 ± 0.0.04, and 3.6 ± 0.27 at –48, –36, and –24 mV, respectively.

TWIK-2 was the sixth K_{2P} to be discovered and has been designated as *KCNK*6 (13–16). Of the K_{2P} family members, TWIK-2 is most closely related to TWIK-1 (*KCNK*1) and the non-functional protein coded by gene, *KCNK*7 (21). In the rat, TWIK-2 is expressed in lung, pancreas, placenta, kidney, spleen, heart, esophagus, stomach, colon, and other tissues (21). A similar, but not identical, expression pattern was reported for the human (13–15, 22). Of particular significance to this study, TWIK-2 is expressed in all arteries studied to date including aorta, middle cerebral, pulmonary, and mesenteric arteries (3, 6, 7, 13, 14). Multi-cell RT-PCR and/or immunofluorescence studies have indicated that TWIK-2 is expressed in smooth muscle (6, 7) and possibly the endothelium (7). We have found that a mouse cerebrovascular endothelial cell line (bEnd.3 from ATCC) expresses TWIK-2 message (unpublished observation).

Our long range goal is to determine the function of TWIK-2 in the vascular system. Since there are no selective inhibitors or activators for TWIK-2, we decided to clone TWIK-2 from the rat middle cerebral artery, characterize its channel properties, and determine if currents from the cloned channel resemble currents that we previously obtained from freshly isolated VSM cells from rat middle cerebral artery (6).

One problem that we and others have encountered involved identifying cells in which TWIK-2 was inserted into the plasma membrane (15, 16). In order to overcome this problem, we expressed GFP -rTWIK-2 in the CHO cells. Having the GFP marker allowed us to discriminate between cells that did not express TWIK-2, cells that expressed TWIK-2 but did not insert the channel into the membrane, and cells that expressed and inserted TWIK-2 in the plasma membrane. While the use of GFP -rTWIK-2 is a potential limitation of this study, it did provide unequivocal identification of those cells, used for whole cell recordings, where the rTWIK-2 was in the plasma membrane.

TWIK-2 currents, cloned from the rat middle cerebral artery (this study), showed properties that were both similar and different from previous studies (13, 14). Our studies demonstrated that rat rTWIK-2-GFP currents were relatively linear in physiological K^+ concentrations but become slightly inwardly rectifying in symmetrical K^+ (Figs. 2 and 3). The currents were weakly inactivating at the more positive potentials (Fig. 2A). These results were similar, but not identical, to those previously published for rat and human TWIK-2 (13). Chavez *et al*. reported that human TWIK-2 expressed in oocytes were non-inactivating and inwardly rectifying at all concentrations of extracellular K^+ (14). rTWIK-2-GFP cloned from the rat middle cerebral artery was insensitive to 10 mM TEA, 3 mM 4-aminopyridine, and 10 μM glibenclamide (Figs. 4A and B). These results are consistent with other studies (13, 14). TEA, glibenclamide, and 4-aminopyridine are inhibitors of Ca^{2+}-activated, ATP-sensitive, and voltage-gated K channels, respectively.

rTWIK-2-GFP was inhibited by Ba^{2+} having an IC_{50} near 80 μM (Figs. 5 and 6). This inhibition by Ba^{2+} was in good agreement with Patel *et al*. (13) who reported an IC_{50} for Ba^{2+} of 100 μM. In addition, Patel *et al*. reported that 10 μM arachidonic acid increased currents by 76% (13); Chavez reported that the same concentration of arachidonic acid had no effect on TWIK-2 (14). Our studies showed that rTWIK-2-GFP could be activated by arachidonic acid but a concentration of 100 μM is required (Fig. 7).

A major thrust of this study was to begin an investigation of the role for TWIK-2 in rat vascular smooth muscle. Therefore, we compared TWIK-2 currents from the cloned channel (this study) to native currents previously reported for rat middle cerebral artery VSM cells (6). The currents in freshly isolated VSM can be characterized as outwardly rectifying. Almost all of the resting current in VSM was blocked with 10 mM TEA (6), a concentration that did not affect cloned rTWIK-2-GFP channels (Fig. 4A). Thus, the contribution of TWIK-2 to the resting K^+ currents would be either minimal or non-existent.

We previously showed that in the presence of 10 mM TEA, 10 μM arachidonic acid elicited large outwardly rectifying currents. This current was not blocked by 4-aminopyridine, glibenclamide, or Ba^{2+} (100 μM) (6). One possibility for the arachidonic acid-sensitive current was activation of TWIK-2 (6). However, the present study casts doubts on this possibility. First, the arachidonic acid-stimulated currents in VSM were outwardly rectifying (6). Cloned rTWIK-2-GFP showed a linear current (Fig. 2). Second, the arachidonic acid-sensitive current in VSM could be elicited by 10 μM arachidonic acid (6). Cloned rTWIK-2-GFP currents required a ten-fold greater concentration of arachidonic acid (i.e., 100 μM) for activation (Fig. 7). And third, the arachidonic acid-sensitive currents in VSM were insensitive to 100 μM Ba^{2+}. According to the

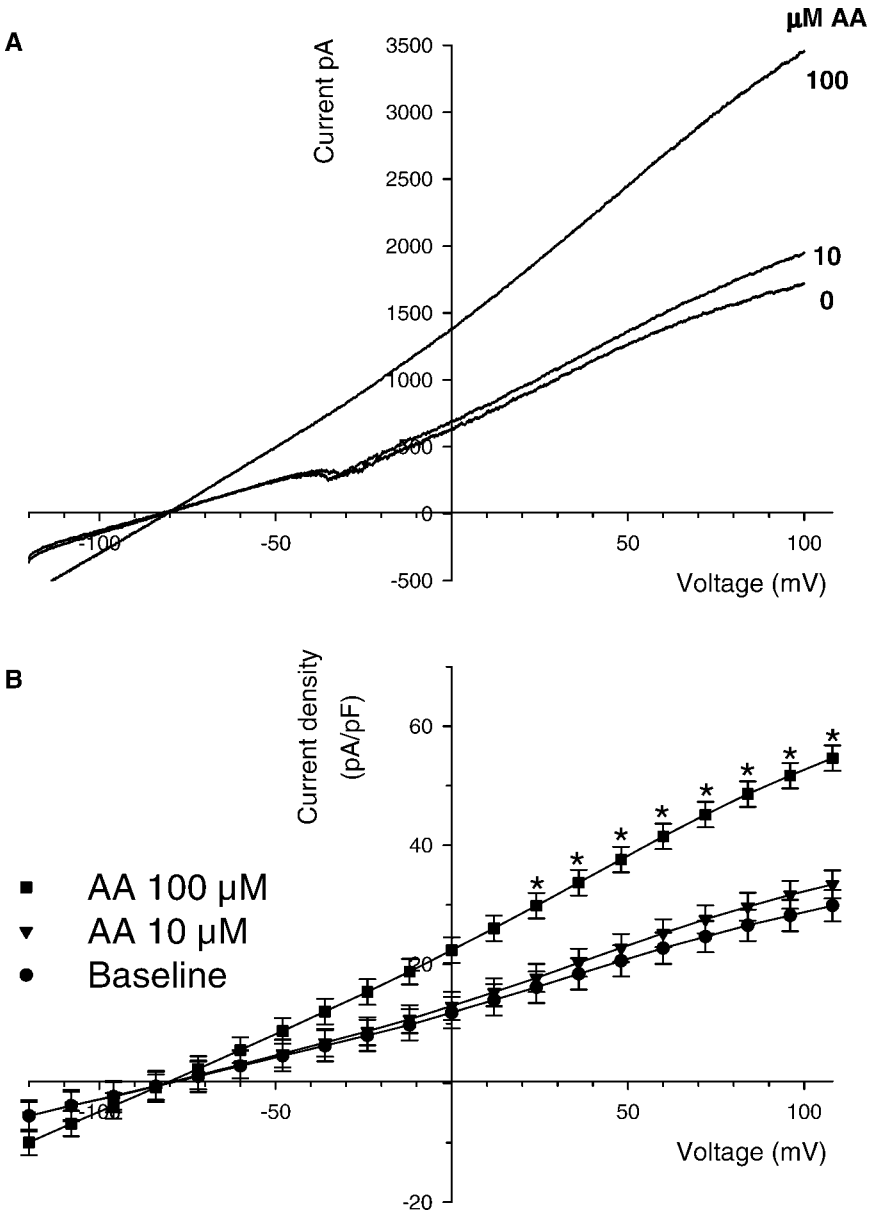

Figure 7. (A) The effect of arachidonic acid (AA) on the rTWIK-2-GFP current in a single CHO cell. (B) Summary data for the effect of arachidonic acid on rTWIK-2-GFP currents ($n = 4$–6). * $P < 0.05$ compared to baseline.

cloned channel, over 50% of the rTWIK-2-GFP current should have been blocked if arachidonic acid was activating TWIK-2 in VSM (Figs. 5 and 6). These three lines of evidence indicate that TWIK-2 was not responsible for the arachidonic acid-sensitive currents in freshly isolated VSM from rat middle cerebral artery.

A comparison of currents from the cloned channel to native currents in freshly isolated VSM of the rat middle cerebral did not provide any clues as to the function of TWIK-2. However, it must be emphasized that the search for the functional role of TWIK-2 has only begun. There are two factors that are worth discussing in this context. First, it is possible that we have not looked at conditions in VSM where TWIK-2 is activated. With this scenario, TWIK-2 would be inactive until an appropriate response occurs in the VSM. This could be stimulation of a pathway that activates TWIK-2 or inhibition of a pathway which inhibits channel activity. Second, the studies of cloned TWIK-2 and native currents were conducted at room temperature. It is possible that TWIK-2-like currents would have been seen in VSM if the studies had been conducted at a temperature at or near the normal physiological temperature of 37°C.

While we were unable to link TWIK-2 with a known function, we were able to narrow the search by ruling out some possibilities. Given that there are no selective activators or inhibitors for TWIK-2 at the present time, a good strategy for determining a functional role would be to

knock the channel down with antisense or RNAi, or to generate a TWIK-2 knockout mouse.

1. Jackson WF. Potassium channels in the peripheral microcirculation. Microcirculation 12(1):113–127, 2005.
2. Bryan RM Jr, Joseph BK, Lloyd E, Rusch NJ. Starring TREK-1: the next generation of vascular K+ channels. Circ Res 101(2):119–121, 2007.
3. Gurney A, Manoury B. Two-pore potassium channels in the cardiovascular system. Eur Biophys J 38:305–318, 2009.
4. Brayden JE, Quayle JM, Standen NB, Nelson MT. Role of potassium channels in the vascular response to endogenous and pharmacological vasodilators. Blood Vessels 28:147–153, 1991.
5. Nelson MT, Quayle JM. Physiological roles and properties of potassium channels in arterial smooth muscle. Am J Physiol Cell Physiol 268:C799–C822, 1995.
6. Bryan RM Jr, You J, Phillips SC, Andresen JJ, Lloyd EE, Rogers PA, *et al*. Evidence for two-pore domain potassium channels in rat cerebral arteries. Am J Physiol Heart Circ Physiol 291(2):H770–H780, 2006.
7. Gardener MJ, Johnson IT, Burnham MP, Edwards G, Heagerty AM, Weston AH. Functional evidence of a role for two-pore domain potassium channels in rat mesenteric and pulmonary arteries. Br J Pharmacol 142(1):192–202, 2004.
8. Blondeau N, Petrault O, Manta S, Giordanengo V, Gounon P, Bordet R, *et al*. Polyunsaturated fatty acids are cerebral vasodilators via the TREK-1 potassium channel. Circ Res 101(2):176–184, 2007.
9. Garry A, Fromy B, Blondeau N, Henrion D, Brau F, Gounon P, *et al*. Altered acetylcholine, bradykinin and cutaneous pressure-induced vasodilation in mice lacking the TREK1 potassium channel: the endothelial link. EMBO Rep 8(4):354–359, 2007.
10. Gonczi M, Szentandrassy N, Johnson IT, Heagerty AM, Weston AH. Investigation of the role of TASK-2 channels in rat pulmonary arteries; pharmacological and functional studies following RNA interference procedures. Br J Pharmacol 147(5):496–505, 2006.
11. Gurney AM, Osipenko ON, MacMillan D, McFarlane KM, Tate RJ, Kempsill FEJ. Two-pore domain K channel, TASK-1, in pulmonary artery smooth muscle cells. Circ Res 93(10):957–964, 2003.
12. Olschewski A, Li Y, Tang B, Hanze J, Eul B, Bohle RM, *et al*. Impact of TASK-1 in human pulmonary artery smooth muscle cells. Circ Res 98(8):1072–1080, 2006.
13. Patel AJ, Maingret F, Magnone V, Fosset M, Lazdunski M, Honore E. TWIK-2, an inactivating 2P domain K+ channel. J Biol Chem 275(37): 28722–28730, 2000.
14. Chavez RA, Gray AT, Zhao BB, Kindler CH, Mazurek MJ, Mehta Y, *et al*. TWIK-2, a new weak inward rectifying member of the tandem pore domain potassium channel family. J Biol Chem 274(12):7887–7892, 1999.
15. Pountney DJ, Gulkarov I, Vega-Saenz DM, Holmes D, Saganich M, Rudy B, *et al*. Identification and cloning of TWIK-originated similarity sequence (TOSS): a novel human 2-pore K+ channel principal subunit. FEBS Lett 450(3):191–196, 1999.
16. Salinas M, Reyes R, Lesage F, Fosset M, Heurteaux C, Romey G, *et al*. Cloning of a new mouse two-P domain channel subunit and a human homologue with a unique pore structure. J Biol Chem 274(17):11751–11760, 1999.
17. Baker SA, Hennig GW, Han J, Britton FC, Smith TK, Koh SD. Methionine and its derivatives increase bladder excitability by inhibiting stretch-dependent K(+) channels. Br J Pharmacol 153(6): 1259–1271, 2008.
18. Han J, Gnatenco C, Sladek CD, Kim D. Background and tandem-pore potassium channels in magnocellular neurosecretory cells of the rat supraoptic nucleus. J Physiol 546(Pt 3):625–639, 2003.
19. Salkoff L, Jegla T. Surfing the DNA databases for K+ channels nets yet more diversity. Neuron 15(3):489–492, 1995.
20. Lesage F, Guillemare E, Fink M, Duprat F, Lazdunski M, Romey G, *et al*. TWIK-1, a ubiquitous human weakly inward rectifying K+ channel with a novel structure. EMBO J 15(5):1004–1011, 1996.
21. Goldstein SAN, Bayliss DA, Kim D, Lesage F, Plant LD, Rajan S. International Union of Pharmacology. LV. Nomenclature and molecular relationships of two-P potassium channels. Pharmacol Rev 57(4): 527–540, 2005.
22. Medhurst AD, Rennie G, Chapman CG, Meadows H, Duckworth MD, Kelsell RE, *et al*. Distribution analysis of human two pore domain potassium channels in tissues of the central nervous system and periphery. Brain Res Mol Brain Res 86(1–2):101–114, 2001.